



Air-sea interaction between tropical cyclone Nari and Kuroshio

Chau-Ron Wu,^{1,2} Yu-Lin Chang,¹ Lie-Yauw Oey,² C.-W. June Chang,³ and Yi-Chia Hsin¹

Received 11 March 2008; revised 23 April 2008; accepted 8 May 2008; published 25 June 2008.

[1] The air-sea interaction between tropical cyclone Nari (Sep/6–16/2001) and Kuroshio is studied using satellite observations and an ocean model. Nari crossed the Kuroshio several times, which caused variations in typhoon intensity. Nari weakened when it was over the shelf north of Kuroshio where cooling took place due to mixing of the shallow thermocline. The cyclonic circulation penetrated much deeper for the slowly-moving storm, regardless of Nari's intensity. Near-inertial oscillations are simulated by the model in terms of the vertical displacement of isotherms. The SST cooling caused by upwelling and vertical mixing is effective in cooling the upper ocean several days after the storm had passed. At certain locations, surface chlorophyll-a concentration increases significantly after Nari's departure. Upwelling and mixing bring nutrient-rich subsurface water to the sea surface, causing enhancement of phytoplankton bloom.
Citation: Wu, C.-R., Y.-L. Chang, L.-Y. Oey, C.-W. J. Chang, and Y.-C. Hsin (2008), Air-sea interaction between tropical cyclone Nari and Kuroshio, *Geophys. Res. Lett.*, *35*, L12605, doi:10.1029/2008GL033942.

1. Introduction

[2] Tropical cyclone (TC) Nari (Sep/6–16/2001) is an unusual typhoon; its track is unique to the region. Nari was a moderate category-3 typhoon on the Saffir-Simpson scale. The storm's minimum central pressure was 944 hPa and its maximum wind speed (MWS) was 50 m/s. The storm formed off the northeastern Taiwan at $\sim 25.0^\circ\text{N}$, 124.7°E on Sep/06/00Z (Figure 1). It first moved eastward following a mid-latitude atmospheric trough, turning northwestward and westward after passing Okinawa Island as another typhoon (Danas) approached southern Japan. On Sep/09/00Z, it turned southward and then southeastward to complete a loop. Nari lingered for about 2 days around 26.4°N , 127°E before proceeding northwestward. After Danas moved eastward away from Japan and a weak high pressure system developed over central China, Nari began to move slowly southwestward and finally made landfall at the northern Taiwan coast on Sep/16/18Z. Nari took 94 lives and caused extensive property damage due to the heavy rainfall associated with the storm. Both the air-sea interaction and large-scale atmospheric circulation appear to have

influenced the unique movements and changes in the intensity of Nari [*Sui et al.*, 2002].

[3] Nari remained within a restricted area of the south-eastern East China Sea (ECS) for a long 11-day period. Often a near-stationary typhoon weakens and dissipates because of the lack of the energy supplied by the ocean as the SST cools [*Schade and Emanuel*, 1999]. Nari vacillates about the Kuroshio for about one week. As Figure 1 shows, there appears to be an interesting interaction between the storm and the Kuroshio front. Before Nari's arrival, the southern ECS is characterized by warm sea surface temperatures (SST) above 29°C : this was one of the warmest summers on record based on satellite observations. In addition, Nari intensified as it crossed over the Kuroshio onto the shelf on Sep/7–9, and continued to strengthen as the storm crossed back to the Kuroshio (Sep/10–12). However, on its second crossing onto the shelf, Nari weakened (Sep/13–15).

[4] The importance of air-sea interaction in affecting TC intensity has been previously documented [e.g., *Lin et al.*, 2005; *Wu et al.*, 2007]. TC intensification over the Loop Current and the Gulf Stream has been recognized and studied. *Shay et al.* [2000] noted that sudden intensification may occur when TCs pass over the warm Loop Current or warm eddy in the Gulf of Mexico. However, less is known about the effects of a typhoon on the powerful Kuroshio and their coupling in the Pacific. The wobbling of Nari in the vicinity of Kuroshio appears to cause variations in the typhoon intensity. The interactions between Nari and Kuroshio thus represent one of the most interesting and challenging examples for the air-sea interaction study. In this study, as a first step the response of the Kuroshio and surrounding waters to the passage of typhoon Nari on the southern ECS is investigated using independent satellite observations and a three-dimensional primitive equation ocean model. Since the model resolves temporal and spatial scales of interest, we will use the results to explain the cooling in the upper ocean caused by the upwelling of cooler subsurface waters. We also describe the observed physical and biological responses induced by Nari.

2. Observations and Model

[5] Typhoon Nari information is obtained from the best-track data from the Joint Typhoon Warning Center (JTWC). The cloud-penetrating SST from TRMM/TMI (Tropical Rainfall Measuring Mission, Microwave Imager) is used to study the upper ocean response to Nari. Satellite data also include NASA QSCAT ocean surface wind vectors. The biological response to the passing of Nari is illustrated with chlorophyll-a concentration (Chl-a) from the SeaWiFS sensor (Sea-viewing Wide Field-of-view Scanner).

[6] The East Asian Marginal Seas (EAMS, domain is $99\sim 140^\circ\text{E}$ and $0\sim 42^\circ\text{N}$) model used here is based on the

¹Department of Earth Sciences, National Taiwan Normal University, Taipei, Taiwan.

²Program in Atmospheric and Oceanic Sciences, Princeton University, Princeton, New Jersey, USA.

³Department of Atmospheric Science, National Taiwan University, Taipei, Taiwan.

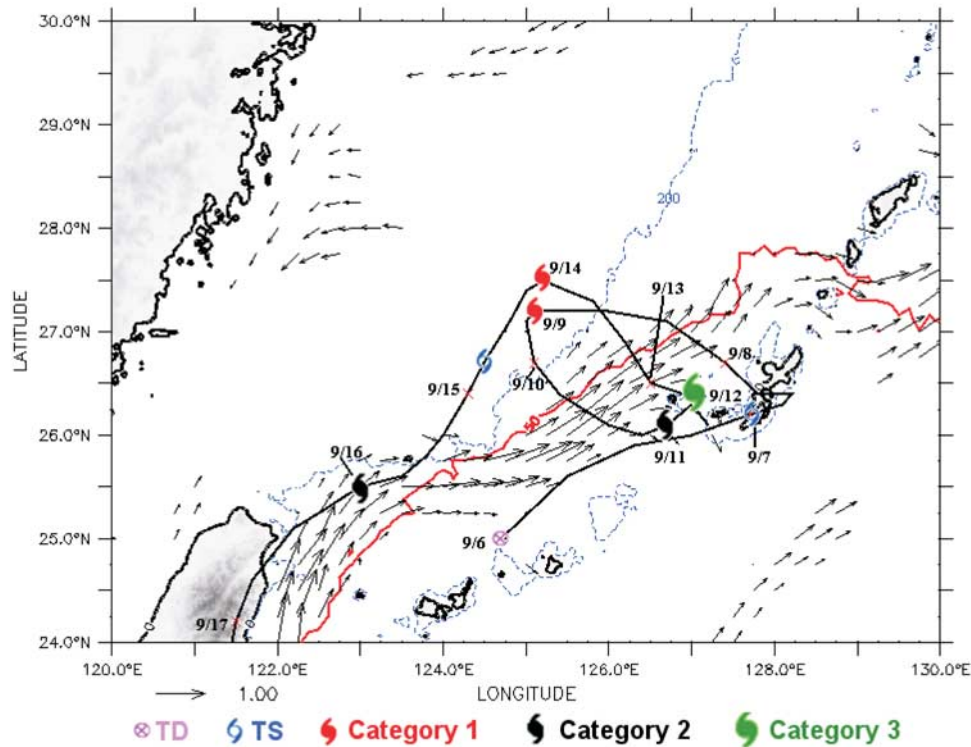


Figure 1. Track and intensity of Nari (thick-black line) together with the modeled Kuroshio velocity field (vectors) where the magnitude larger than 40 cm/s is presented. Thick-red contour indicates OHC = 50 kJ/cm². The 200 m isobath is also overlaid (blue contours).

Princeton Ocean Model (POM) [Mellor, 2004] with realistic topography and forcing at a horizontal resolution of 1/8° embedded in a north Pacific model at 1/4° resolution, also using POM. The EAMS model was continuously run for 26 years from 1980 through 2005, and the period covering typhoon Nari is used in the present study. From 1999 through 2005, the model is forced with QSCAT/NCEP six-hourly wind fields (0.5° × 0.5°) and a quadratic drag formula based on Gill's [1982] formula. Additional information and validation on the EAMS model is given by Wu and Hsin [2005] and Hsin et al. [2008]. The vectors in Figure 1 are the modeled surface velocity fields averaged over Nari's duration from September 6 to 16, 2001. For clarity, only velocities larger than 40 cm/s are presented. The Kuroshio enters the region along the east coast of Taiwan. After leaving Taiwan, it turns eastward at ~25.5°N, 123°E and then northeastward at 125°E, approximately parallel to the 200 m isobath. The general flow patterns from model simulation agree well with earlier findings, such as the annual mean pattern of surface currents derived from GEK (geomagnetic electrokinetograph) data from 1953 to 1984 [Qiu and Imasato, 1990] and also those derived from trajectories of surface drifters from 1989 to 1996 [Lie et al., 1998].

3. Effects of Ocean on Nari

[7] The apparent effect of Kuroshio and adjacent shelf waters on Nari is examined using TMI/SST images (Figure 2)

from September 7 to 17, 2001. The modeled surface velocity fields averaged over Nari's duration are overlaid on the SST images. In pre-typhoon conditions (Sep/7), SST contours roughly parallel the Kuroshio path and are oriented southwest-northeast with lower temperatures near the Chinese coast and higher temperature offshore. A tropical depression off northeastern Taiwan moved northeastward along the Kuroshio. It turned eastward and became a tropical storm near Okinawa Island (Figure 2a). It strengthened and became a category-1 typhoon on Sep/8 as it traversed northwestward over the warm Kuroshio (Figure 2b). Nari strengthened further while it moved southeastward and crossed the Kuroshio again; it slowed down and became a category-3 typhoon on Sep/11/12Z (Figure 2c). Nari weakened and became a category-1 typhoon on Sep/13 when it approached a cold dome, centered at ~27.2°N, 125°E, which was apparently due to upwelling produced by the storm during its first encounter with the shelf water (Figure 2d). On Sep/14/18Z, Nari weakened further and became a tropical storm at ~27°N, 124.6°E (Figure 2e). Subsurface cold waters were entrained up to the sea surface through upwelling and mixing, and the process leads to a decrease in SST that can weaken Nari. The maximum SST cooling occurred on Sep/17 (Figure 2f). The Nari-induced cold SST patch (123.5–126°E, 26.6–29°N) has the dimension of around 250–300 km. The minimum SST of 24.5°C is found in the cold pool center (125°E, 28°N), increasing outwards to ~27.5°C around the periphery. Nari strengthened into a category-2 typhoon as it moved southwestward

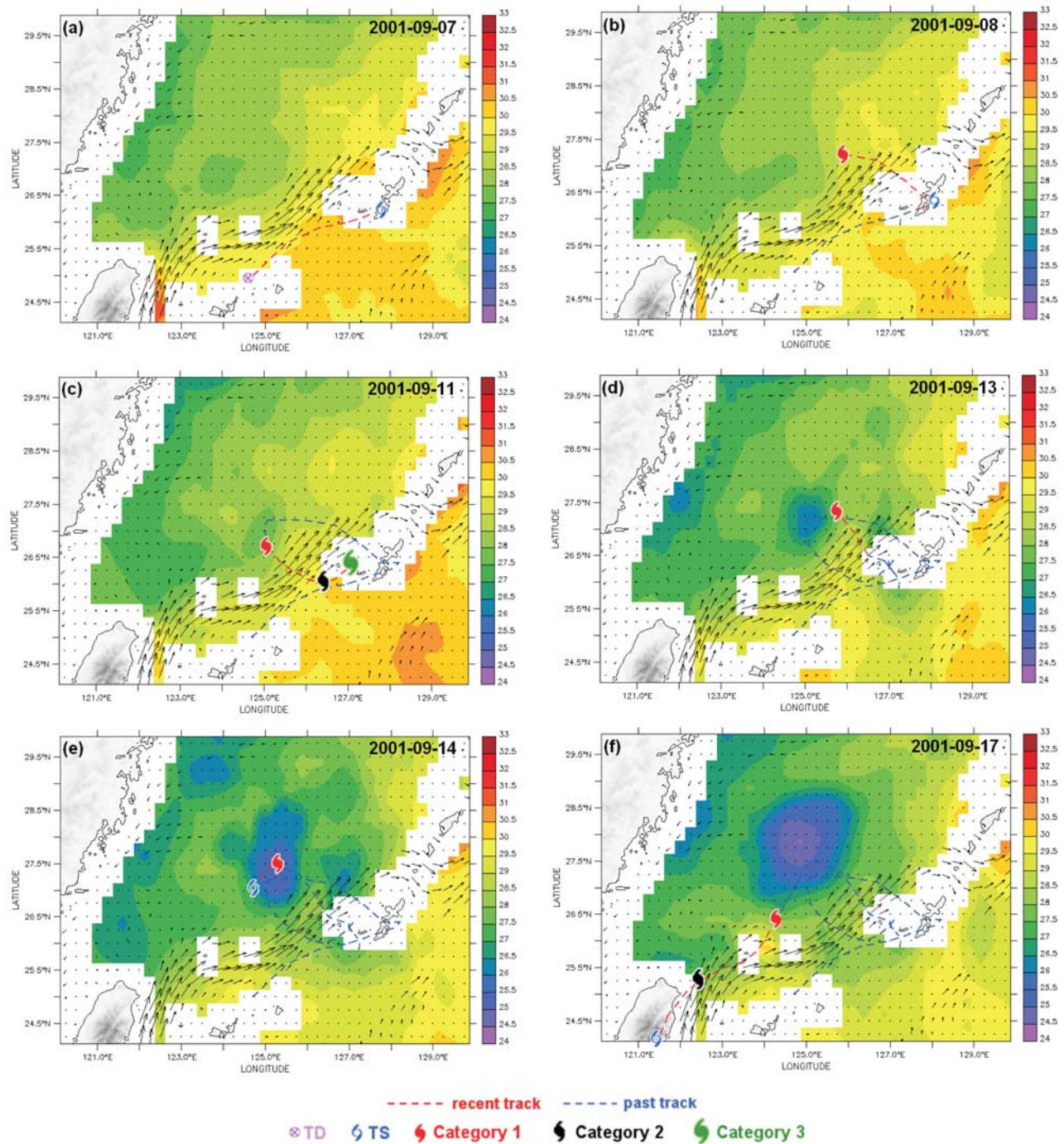


Figure 2. The sequential representative TMI/SST images during the passage of Nari. Typhoon track and modeled Kuroshio averaged over Nari’s duration are overlaid on (a) Sep/07, (b) Sep/08, (c) Sep/11, (d) Sep/13, (e) Sep/14, and (f) Sep/17.

and passed over the warm Kuroshio again on its way to Taiwan (Figure 2f).

4. Oceanic Response Induced by Nari

[8] The oceanic response induced by Nari is investigated using the model simulation. Although the counter-clockwise rotating winds favor divergence of the surface water and upwelling of cooler water from the subsurface, the SST cooling does not occur throughout the trail of Nari. Table 1

lists the location and intensity of Nari together with the SST, local water depth, and the position of Nari relative to the Kuroshio. In addition, information on whether or not a cyclonic eddy is well developed is also provided. A cyclonic eddy is well developed only when Nari is located north of Kuroshio (e.g. on Sep/08/18Z, Sep/09/00Z, Sep/13/12Z, and Sep/14/12Z). In contrast, the cyclonic circulation is diffused, and does not form a well-defined eddy when Nari is located south of, or directly over the Kuroshio.

Table 1. Location and Intensity of Typhoon Nari Together With SST, Local Water Depth, the Corresponding Location Between Nari and Kuroshio, and Whether a Cyclonic Eddy Is Well Developed

	6 Sep	7 Sep	8 Sep	9 Sep	10 Sep	11 Sep	12 Sep	13 Sep	14 Sep	15 Sep
Time	0000Z	0600Z	1800Z	0000Z	1800Z	1800Z	1800Z	1200Z	1200Z	1800Z
Position	124.7°E 25.0°N	128.1° 26.3°N	125.5° 27.2°N	125.1° 27.2°N	126.4° 26.0°N	127.0° 26.4°N	126.9° 26.4°N	125.8° 27.3°N	124.8° 27.1°N	123.5° 25.6°N
Type	TD	TS	C1	C1	C1	C2	C1	C1	C1	C1
MWS (kts)	25	45	65	65	75	95	75	65	65	80
SST (deg C)	-	-	28.5	28.5	29.5	-	-	25.5	27.3	28
Local water depth (m)	1934	530	154	112	1464	1034	677	161	102	732
In relation to Kuroshio	south	south	north	north	above	above	above	north	north	above
Eddy formation	no	no	yes	yes	no	no	no	yes	yes	no

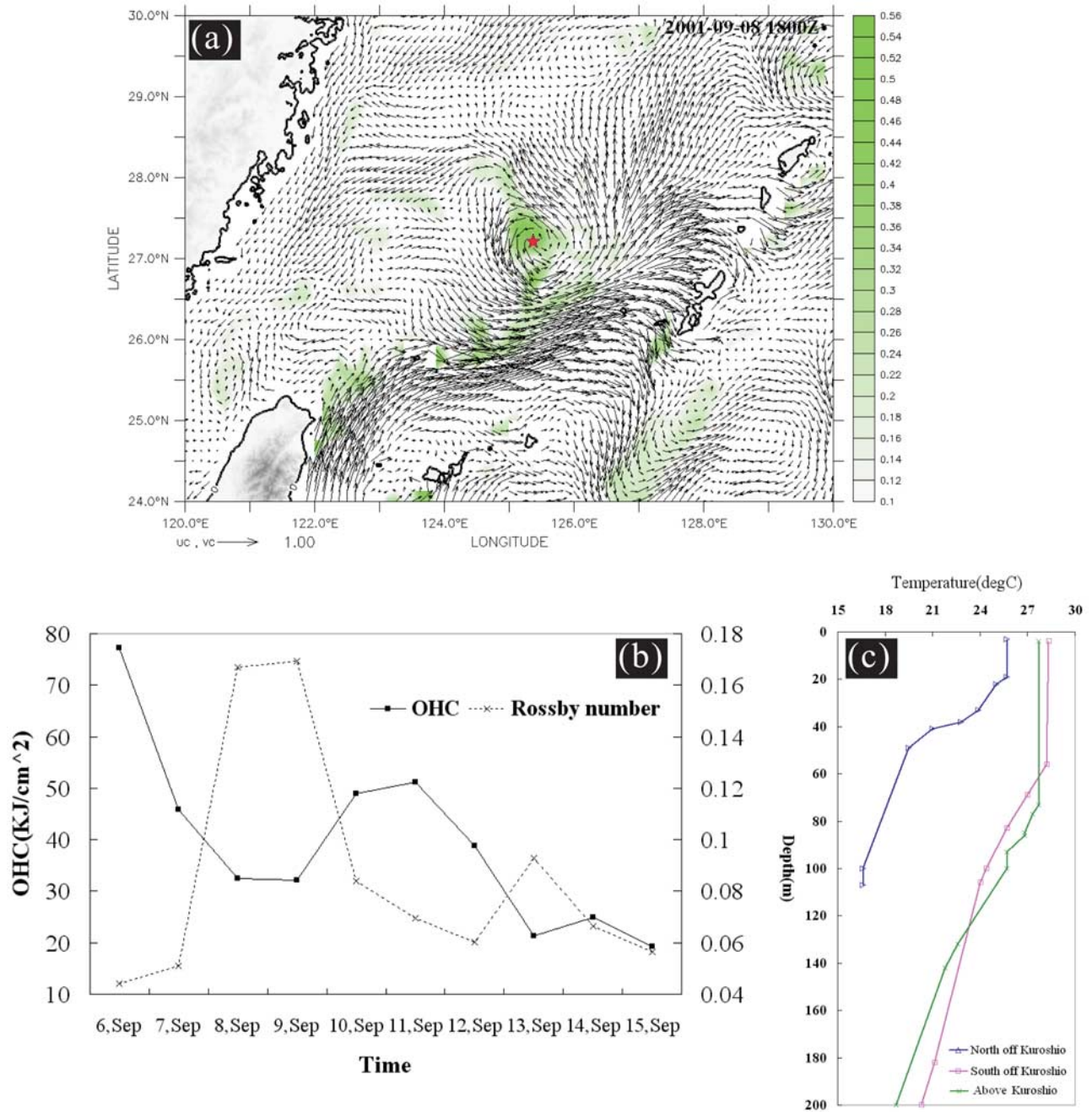


Figure 3. (a) Current velocity vectors and Rossby number (ζ/f , positive values only are shown, green shading) on Sep/08/18Z, (b) the daily OHC (solid squares) together with Rossby number (cross) during Nari’s passage, and (c) GTSP temperature profiles from shelf waters north of Kuroshio (29°N, 125.99°E), south of Kuroshio (25.9°N, 128.15°E), and above Kuroshio (28.16°N, 127.23°E).

Table 2. Rossby Number Around the Cyclonic Eddy Induced by Nari on 8, 9, and 13 September^a

	8 Sep	9 Sep	13 Sep
Time	1800Z	0000Z	1200Z
propagating speed (m/s)	2.22	1.39	2.22
MWS (kts)	65	65	65
local water depth (m)	154	112	161
SST (deg C)	28.5	28.5	25.5
Ro at various depths			
0 m	0.39	0.32	0.11
10 m	0.34	0.28	0
20 m	0.21	0.26	0
30 m	0	0.26	0
50 m	0	0.26	0
75 m	0	0.23	0
100 m	0	0.15	0

^aRossby number $Ro = \zeta/f$.

[9] To further clarify the different response of the Kuroshio and adjacent waters to Nari, the corresponding ocean current velocity and Rossby number are depicted in Figure 3a, when Nari was situated north of Kuroshio. In general, the surface winds near the storm's eye are weaker while the surrounding wind speed is much stronger. The cyclonic circulation of current vectors is clearly found near the center of the storm when Nari is at $\sim 27.2^\circ\text{N}$, 125.5°E north of the Kuroshio on Sep/08/18Z. The significant positive vorticity is also evident and co-located with the counter-clockwise rotating surface winds. On Sep/11/18Z, Nari is centered at $\sim 26.1^\circ\text{N}$, 127°E near the Okinawa Island south of the Kuroshio; although the storm intensify into a category-2 typhoon with a much stronger MWS there is no clear cyclonic circulation and significant positive vorticity (figure not shown). Apparently, the presence of Okinawa Island prevents the development of the positive vorticity and the formation of a cyclonic eddy. Nari is directly over the Kuroshio on Sep/15/18Z, but there is again no significant positive vorticity and the evidence of a cyclonic eddy (figure not shown). The strong currents and vorticity of the Kuroshio may prevent the development of the cyclonic circulation. The Kuroshio has a much deeper thermocline, and cooling due to upwelling is lessened (see the Discussion section for details). Also, heat is continually being replenished from the south by strong advection. These processes together explain why there is no significant SST cooling observed near the Kuroshio axis after Nari's departure (Figure 2f).

[10] The vorticity structure around the cyclonic eddy induced by Nari has also been studied. On September 8, 9, and 13, the cyclonic circulation pattern in the surface ocean is evident (Table 1). Although the typhoon intensity is about the same these days when the MWS was 65 kts (~ 35 m/s), the cyclonic eddy was found above the depth of 20 m on Sep/08/18Z and at the sea surface on Sep/13/12Z, whereas it penetrates to the entire ocean depth on Sep/09/00Z (Table 2). The propagation speed, U , of the storm is responsible for the phenomenon. Nari has a propagation speed of 2.2 m/s on both Sep/08 and Sep/13, but it slowed down on Sep/09 with a propagation speed of 1.4 m/s. The first-mode baroclinic phase speed, C , computed from the observed temperature and salinity profiles from National Oceanographic Data Center (NODC) is 2.2 m/s, so that Nari was subcritical ($U/C < 1$) on Sep/09 and near-critical or

supercritical ($U/C > 1$) on Sep/08 and Sep/13. The deeper influence depth on Sep/09 suggested by our model is consistent with the theoretical expectation that localized upwelling is prevalent under a subcritical storm whereas a wave-like pattern of alternating upwelling and downwelling cells are left behind a supercritical storm [Geisler, 1970; Price, 1981].

5. Discussion

[11] During the passage of Nari, the significant SST cooling took place only in shelf and slope regions north of the Kuroshio where the water depths are around 100–170 m. The cooling in the upper ocean is in part caused by mixing as well as upwelling of the subsurface cooler water. Figure 3b shows daily ocean heat content (OHC) [Leipper and Volgenau, 1972] and Rossby number ($Ro = \zeta/f$) near 27.2°N , 125.5°E (indicated by an asterisk in Figure 3a) from the model simulation. The OHC tends to decrease whenever Ro peaks, indicating that significant cooling of near-surface water during those dates (on September 8, 9, and 13). The strongest sea surface cooling is observed to the north of the Kuroshio where Nari had already weakened, which suggests that the significant vertical mixing is not wholly associated with Nari's MWS or initial SST (see Table 1). Rather, the significant cooling is also caused by the shallower thermocline that existed on the shelf prior to Nari. No observed temperature profiles exist during the period of the storm, but from October 6 to 8, 2001, three temperature profiles in the region from GTSP (Global Temperature-Salinity Profile Program) are available and are shown in Figure 3c. The thermocline is shallow (20–30 m) north of the Kuroshio over the shelf; it is deep (80–100 m) over and south of the Kuroshio. Thus cool waters beneath the thermocline are closest to the sea surface on the shelf, and typhoon-induced vertical mixing would be expected to reduce the SST more effectively than in regions where the thermocline is deeper.

[12] Internal waves were also generated after Nari's departure, as seen from the large vertical displacement of the thermocline simulated by the model. Temporal variation of water temperature at a fixed location (indicated by an asterisk in Figure 3a) is characterized by near-inertial oscillations. The period estimated from the model is ~ 26 hours in agreement with the theoretical value at a latitude of 27.2°N .

[13] The SeaWiFS ocean color sensor has been suggested as a feasible tool in quantifying the contribution from TCs for enhanced ocean primary production. For example, Lin *et al.* [2003] indicated that the contribution of TCs to the annual new production in the South China Sea may reach as much as 20–30%. The biological response to the passage of Nari is also observed in the present study. The pre-typhoon condition is illustrated in the SeaWiFS image composite (August 5–28) of surface Chl-a with a concentration of about 0.2 mg/m³ in the study region (Figure 4a). After Nari's passage, a significant increase of surface Chl-a concentration, up to 1.0 mg/m³ is visible in the SeaWiFS composite (September 6–29) (Figure 4b). The maximum surface Chl-a concentration of 1.0 mg/m³ occurred on Sep/14 at $\sim 28^\circ\text{N}$, 125°E . It is centered near the maximum SST cooling, revealed by TMI (Figure 2f). The following sequence of

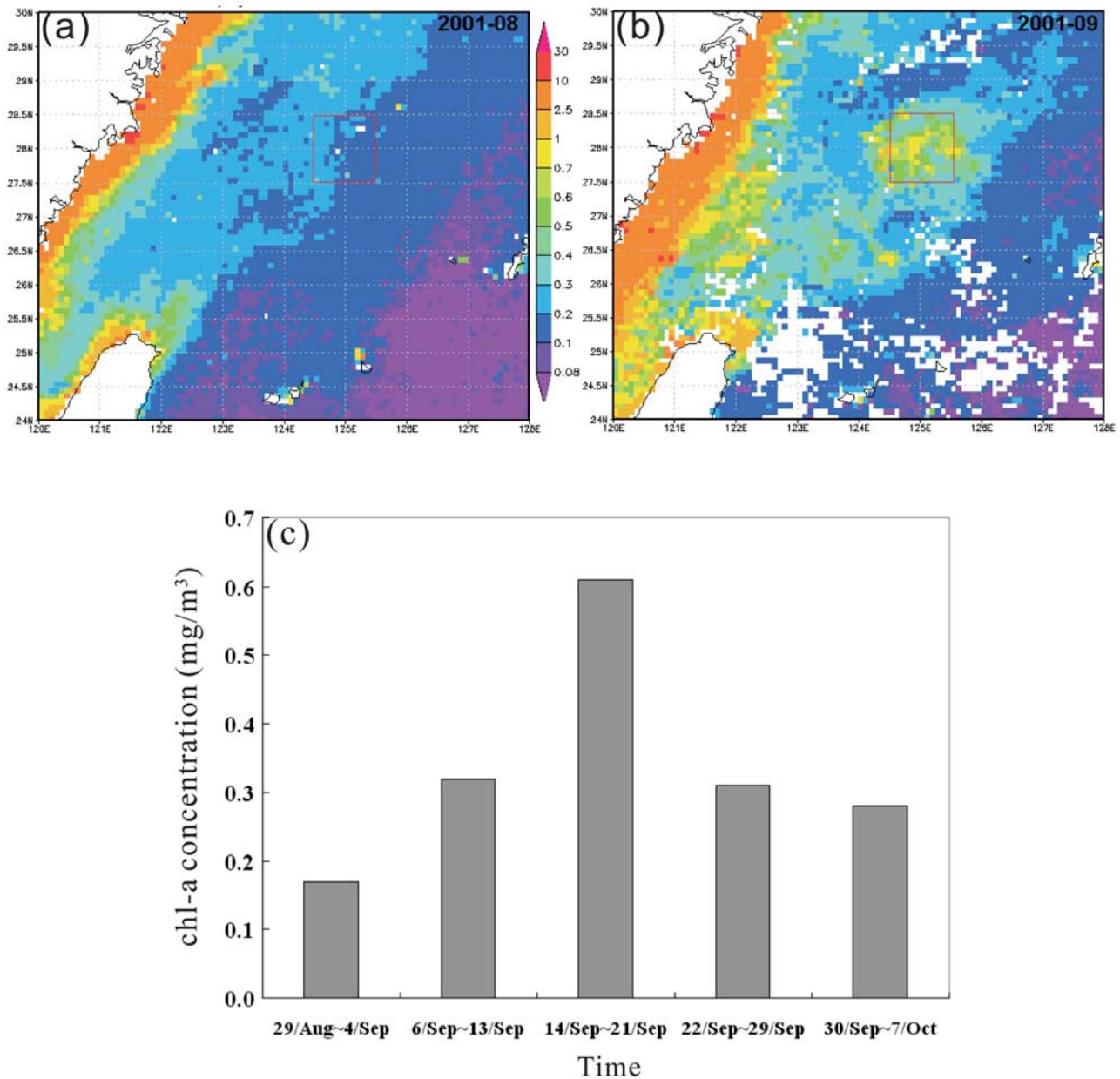


Figure 4. (a) The SeaWiFS composite of Chl-a in mg/m^3 from August 5–28, 2001 before Nari arrival, (b) the SeaWiFS image composite from September 6–29, 2001 after Nari departure, and (c) the temporal variations of chlorophyll-a concentration averaged over the red box in Figure 4b.

events may be inferred: the large and positive vorticity was associated with the strong counter-clockwise rotating TC surface winds on September 8, 9 and 13 during Nari's arrival. The maximum SST cooling occurred a few days later on Sep/16. The combined action of upwelling and mixing brings cold and nutrient-rich water from deeper layers to the sea surface, and significantly increases the surface Chl-a concentration (Figure 4c).

6. Conclusion

[14] Typhoon Nari circled around the Kuroshio over a region off the outer-slope and shelf of the ECS for a period of about 11 days. We find that Nari strengthened as it passed

over the warm Kuroshio, and weakened when it was over the ECS shelf where a cold dome was induced as revealed by TMI/SST. At certain locations along the typhoon track, surface cooling of up to 5°C is observed after Nari's departure. Model simulation indicates that positive vorticities and cyclonic current vectors do not occur throughout the trail of Nari. Only regions north of Kuroshio provide a favorable condition for the development of the cyclone. The cool water north of Kuroshio is maintained for longer than a week. The conditions are very different near the Kuroshio axis, where the water temperatures are restored to their pre-storm values much faster. The model results also confirm that the cyclonic circulation penetrates much deeper for a slow-moving storm regardless of the typhoon intensity.

[15] After typhoon's departure, near-inertial oscillations with period of about 26 hours are simulated by the model in terms of the vertical displacement of isotherms. The SST cooling is caused by upwelling of the cooler subsurface water and vertical mixing. After Nari's passage, the SeaWiFS image composite illustrates a clear enhancement of phytoplankton bloom. This enhancement is a result of the upwelling and mixing which bring subsurface nutrient-rich water to the sea surface.

[16] The present study is a first step to investigate the response of the Kuroshio to the passage of a tropical cyclone. The results given here suggest a close air-sea coupling between typhoon Nari and the Kuroshio. Future plans include research into these coupled physics using both a tropical cyclone model [e.g., Wu *et al.*, 2007] coupled to our high-resolution ocean model, as well as studies into the effects of the coupling with the adjacent shelf-slope waters.

[17] **Acknowledgments.** The invaluable comments from C.-C. Wu and I.-I. Lin of National Taiwan University, and also from the reviewers greatly improved the manuscript. This work is supported by the National Science Council, Taiwan, ROC, under grant NSC 95-2611-M-003-001-MY3.

References

- Geisler, J. E. (1970), Linear theory of the response of a two-layer ocean to a moving hurricane, *Geophys. Fluid Dyn.*, *1*, 249–272.
- Gill, A. E. (1982), *Atmosphere-Ocean Dynamics*, 662 pp., Academic, New York.
- Hsin, Y.-C., C.-R. Wu, and P.-T. Shaw (2008), Spatial and temporal variations of the Kuroshio east of Taiwan, 1982–2005: A numerical study, *J. Geophys. Res.*, *113*, C04002, doi:10.1029/2007JC004485.
- Leipper, D. E., and D. Volgenau (1972), Hurricane heat potential of the Gulf of Mexico, *J. Phys. Oceanogr.*, *2*, 218–224.
- Lie, H.-J., C.-H. Cho, J.-H. Lee, P. Niiler, and J.-H. Hu (1998), Separation of the Kuroshio water and its penetration onto the continental shelf west of Kyushu, *J. Geophys. Res.*, *103*, 2963–2976.
- Lin, I., W. T. Liu, C. Wu, G. T. F. Wong, C. Hu, Z. Chen, W. Liang, Y. Yang, and K. Liu (2003), New evidence for enhanced ocean primary production triggered by tropical cyclone, *Geophys. Res. Lett.*, *30*(13), 1718, doi:10.1029/2003GL017141.
- Lin, I.-I., et al. (2005), The interaction of Supertyphoon Maemi (2003) with a warm ocean eddy, *Mon. Weather Rev.*, *133*, 2635–2649.
- Mellor, G. L. (2004), Users guide for a three-dimensional, primitive equation, numerical ocean model, 56 pp., Program in Atmos. and Oceanic Sci., Princeton Univ., Princeton, N. J.
- Price, J. F. (1981), Upper ocean response to a hurricane, *J. Phys. Oceanogr.*, *11*, 153–175.
- Qiu, B., and N. Imasato (1990), A numerical study on the formation of the Kuroshio Counter Current and the Kuroshio Branch Current in the East China Sea, *Cont. Shelf Res.*, *10*, 165–184.
- Schade, L. R., and K. A. Emanuel (1999), The ocean's effect on the intensity of tropical cyclones: Results from a simple coupled atmosphere-ocean model, *J. Atmos. Sci.*, *56*, 642–651.
- Shay, L. K., G. J. Goni, and P. G. Black (2000), Effects of a warm oceanic feature on Hurricane Opal, *Mon. Weather Rev.*, *128*, 1366–1383.
- Sui, C.-H., et al. (2002), Meteorology-hydrology study targets Typhoon Nari and Taipei flood, *Eos Trans. AGU*, *83*(24), 265.
- Wu, C.-C., C.-Y. Lee, and I.-I. Lin (2007), The effect of the ocean eddy on tropical cyclone intensity, *J. Atmos. Sci.*, *64*, 3562–3578.
- Wu, C.-R., and Y.-C. Hsin (2005), Volume transport through the Taiwan Strait: A numerical study, *Terr. Atmos. Oceanic Sci.*, *16*(2), 377–391.
- C.-W. J. Chang, Department of Atmospheric Science, National Taiwan University, Taipei 11677, Taiwan.
- Y.-L. Chang, Y.-C. Hsin, and C.-R. Wu, Department of Earth Sciences, National Taiwan Normal University, 88, Section 4 Ting-Chou Road, Taipei 11677, Taiwan. (cww@ntnu.edu.tw)
- L.-Y. Oey, Program in Atmospheric and Oceanic Sciences, Princeton University, Princeton, NJ 08544, USA.